THE COLD WORK OF FORMING EFFECT IN STEEL STRUCTURAL MEMBERS

Tian Gao and Cristopher D. Moen

The Charles E. Via, Jr. Department of Civil and Environment Engineering, Virginia Tech
e-mails: gaot@vt.edu, cmoen@vt.edu

Keywords: Cold-Formed Steel, Residual Stresses, Isotropic Hardening, Kinematic Hardening.

Abstract. *A finite element parameter study was conducted to explore the influence of cold bending on steel column load-deformation response. Residual stresses and effective plastic strains, calculated by hand with a recently introduced mechanics-based approach, were input into finite element simulations to define the column's initial state, including the increased yield stress from strain hardening. The column was then loaded to failure in compression with either an isotropic or combined isotropic-kinematic plasticity law. The model with isotropic hardening led to an increased apparent yield stress and a higher column capacity when compared to the baseline case of ignoring cold bending effects. The load-deformation response for the model with a combined isotropic-kinematic hardening law was almost identical to the baseline case, an unexpected result, where the increased yield stress from strain hardening was negated by the shifted Mises yield surface, i.e. the Bauschinger effect. The study highlights an inconsistency in common finite element modeling protocols and design approaches, which rely on the increased yield stress from cold bending for extra capacity without considering residual stresses or kinematic hardening.*

1 INTRODUCTION

Cold bending is a versatile and cost effective fabrication technique for achieving desired structural shapes and geometries. Composite floor beams are cold cambered to accommodate dead load deflections[1-2] (figure 1a). Steel plates are cold bent and welded to form HSS structural sections (figure 1b) [3]. Thin-walled steel columns and joists are manufactured for residential and commercial construction markets by roll-forming flat steel sheet fed from a coil (figure 1c). For all of these applications, the concept of cold bending is the same - apply brute force to yield the steel, and then release the force to achieve a new, permanently deformed shape.

(a) (b) (c)

Figure 1: Cold bending applications: (a)floor beams (photo courtesy of Hydradyne Hydraulics), (b) HSS columns (photo courtesy UTSK Tube Company), (c) light gauge (photo courtesy of Bradbury Group).

When steel is cold-worked, i.e. stretched or compressed above its proportional limit, the steel yield stress increases and ductility (area under the stress-strain curve) decreases due to restrained dislocation mobility in steel's polycrystalline microstructure [4]. Cold bending also results in residual stresses resulting from the imbalance between the partially plastic stress distribution and the elastic stress distribution from unloading (figure 2) [5]. The existence of cold bending residual stresses has been confirmed with experimental measurements at the bent corners of square cold-formed HSS sections [6] and Cee-sections [7-8] and in roller-bent wide flange structural steel beams [9]. Experimental results are supported by computation simulations of cold bending which demonstrate nonlinear residual stress distributions through the depth (thickness) of the member [10].

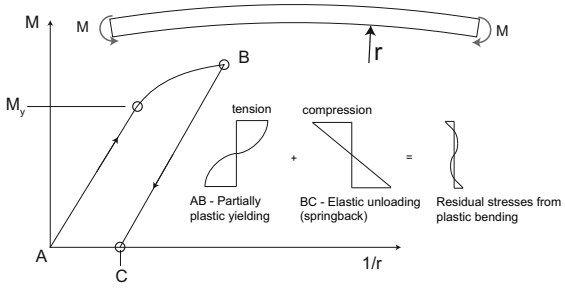

Figure 2: Residual stresses imposed by cold bending.

The mechanics surrounding cold bending are complex, and their treatment in research and design is often inconsistent. Some researchers have observed that nonlinear finite element simulations match experimental results most consistently when cold bending is ignored [11] while others recommend modeling protocols that include residual stresses and an increased yield stress at the cold-bent locations of a member cross-section [12]. The American Iron and Steel Institute (AISI) North American Specification for the Design of Cold-Formed Steel Structural Members [13] allows for increased member capacity based on the 'cold work of forming effect' [14] with empirically derived equations from tests on strain hardened tensile coupons [4], however the presence of residual stresses is not explicitly considered or discussed. The inconsistent treatment of cold bending is at least partially rooted in the mathematical complexity of plasticity-based residual stress predictions [15-16] which limit practical implementation.

The research described herein utilizes finite element simulations to describe in accessible terms how cold bending influences structural behavior. The mechanics that define cold bending residual stresses and plastic strains are introduced, including classical metal plasticity laws, e.g. isotropic and kinematic hardening, which play an important role in simulating structural behavior including the influence of cold bending. Parameter studies are performed on a cold-bent compression member to study how plastic strains and residual stresses affect load-deformation response. Several different treatments are compared, ranging from the baseline case of ignoring the effects of cold bending to implementing metal plasticity and defining residual stresses and plastic strains as part of a member's initial state. The results from this study can be used by researchers to make informed decisions regarding their nonlinear finite element modeling protocols and can guide future code revisions toward a more accurate account of the cold-work of forming effect in design.

2 RESIDUAL STRESSES AND PLASTIC STRAINS FROM COLD BENDING

At the location of cold-bending, residual stresses develop in the direction of the applied bending moment, i.e. the *X*-direction in figure 3. The nonlinear stress distribution is self-equilibrating for axial force and moment through the thickness. Residual stresses also develop in the longitudinal *Z*-direction from the plane strain conditions for a member that is long relative to its width [17]. (Note that the

direction of loading in service is also typically the Z-direction.) A recently introduced mechanics-based prediction method provides hand calculations that can approximate the magnitude and shape of the residual stress and plastic strain distributions for sheet steel or plate [18].

Commercial finite element programs allow a user to input residual stress and plastic distributions as part of the model's initial state. In ABAQUS [19], the cold bending residual stresses σ_1 and σ_3 can be defined at section points through the thickness of shell elements. (Note that σ_2 is assumed equal to zero, see [18].) The effective plastic strain, ε_p, is input in von Mises strain space and defines the magnitude of preexisting strain hardening (figure 3) from cold bending.

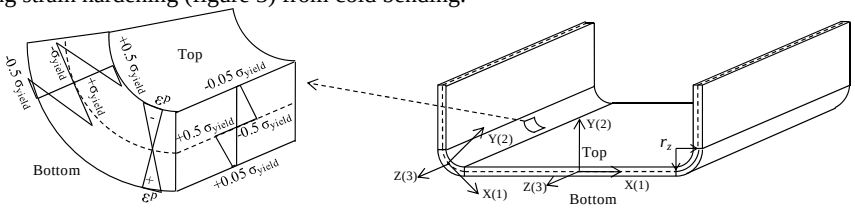

Figure 3: Residual stresses and plastic strains in a cold-bend region of a steel plate or sheet.

3 METAL PLASTICITY LAWS: ISOTROPIC VERSUS KINEMATIC HARDENING

The choice of metal plasticity theory implemented in a finite element model determines how user input residual stresses and plastic strains from cold bending are interpreted. There are two common types of metal plasticity laws available in commercial finite element codes, isotropic or kinematic hardening. Both plasticity laws are defined in the von Mises stress space and are applicable to ductile metals such as steel [20]. Isotropic hardening is typically implemented for a single loading condition, i.e. compressing a column to failure, while kinematic hardening is useful for simulating cyclic loadings or combining different loading states, e.g., cold bending followed by loading to collapse.

3.1 Isotropic Hardening

Isotropic hardening is represented with an expansion of the von Mises ellipsoid as the effective stress, σ_e, exceeds the yield stress, σ_{yield} (figure 4), where:

$$\sigma_e = \frac{1}{\sqrt{2}}\sqrt{(\sigma_1-\sigma_2)^2+(\sigma_2-\sigma_3)^2+(\sigma_3-\sigma_1)^2}\,. \qquad (1)$$

When steel is cold bent, it follows OAB and then springs back along BR as shown in figure 4a and figure 4b. The slope of the lines in figure 4b is equal to Poisson's ratio, v, which is assumed equal to 0.30 for elastic deformation and 0.50 for plastic deformation. The presence of residual stresses after cold bending is denoted with the offset of point R from the origin.

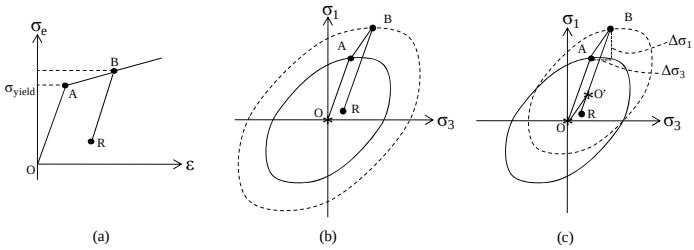

Figure 4: Hardening with residual stresses from cold bending: (a) stress-strain curve, (b) isotropic hardening with expanding yield surface, and (c) kinematic hardening with shifting yield surface.

3.2 Kinematic Hardening

Kinematic hardening is defined with the same von Mises ellipsoid employed for isotropic hardening. However as the stresses exceed σ_{yield} along AB in figure 4c, the center of the yield surface permanently shifts to accommodate the imposed stress. The shifting yield surface is a fundamentally different type of yielding behavior than isotropic hardening (figure 4b). The new location of the yield surface is defined by the backstress components $\Delta\sigma_1$ and $\Delta\sigma_3$.

After the yield surface has shifted, unloading occurs elastically along B to R, terminating at a nonzero residual stress. If the steel is now loaded again in the same direction as the original loading (again along the line OA in figure 4c), the apparent yield stress is increased. However, if the steel is loaded in the opposite direction along OA (i.e. $-\sigma_1$ and $-\sigma_3$), the yield surface (dashed ellipsoid) is reached with a lower apparent yield stress. This asymmetric yield behavior has been documented in experiments and is commonly referred to as the Bauschinger effect [4]. It is hypothesized that the cyclic nature of the loadings applied to cold-bend members, initiating with plastic bending, followed by elastic springback, and then applied load in service, requires a combination of isotropic and kinematic hardening to accurately simulate structural behavior. A finite element parameter study follows which explores how the choice of plasticity law and the inclusion or exclusion of residual stresses and effective plastic strains from cold-bending influences load-deformation response.

4 FINITE ELEMENT ANALYSIS OF A COLD-BENT STEEL COLUMN

A parameter study considering residual stresses and metal plasticity was conducted by considering the load-deformation response of a cold-bent steel column obtained with nonlinear finite element analyses in ABAQUS. The column length is 130 mm with a sheet thickness of 2.6 mm and a centerline radius r_z=305 mm. The steel column was modeled with S9R5 nine node reduced integration thin shell elements. All nodes were restrained in the *X*- and *Y*-directions to eliminate buckling. The modulus of elasticity was assumed as 203.4 GPa, and the elastic Poisson's ratio, *v*, as 0.30. The column was loaded from one end with displacement control employing the modified Riks nonlinear solution method [21]. Four analyses were performed to evaluate the influence of hardening laws and residual stresses on load-deformation response as discussed in the following sections.

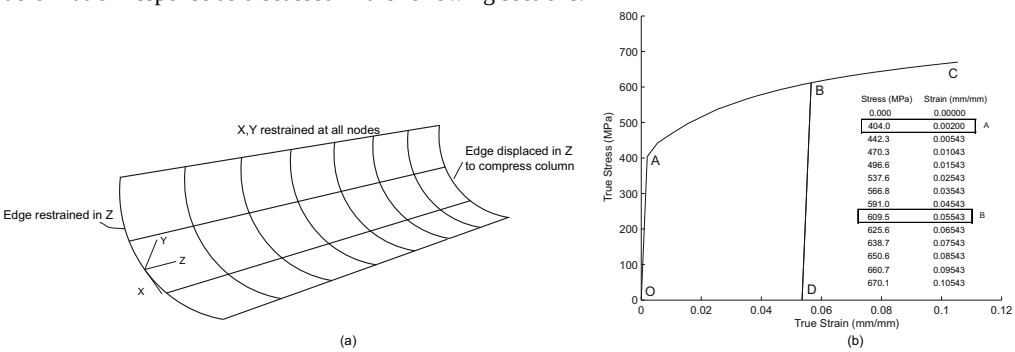

Figure 5: (a) Finite element model boundary conditions and loading and (b) assumed stress-strain curve.

4.1 NORS: Isotropic hardening with virgin stress-strain curve

The baseline case for comparison in this study, NORS, assumes that the effect of cold bending is negligible, i.e. there are no residual stresses present and the virgin yield stress is unchanged. Isotropic hardening was implemented with the true stress-strain curve OABC in figure 5b.

4.2 MAT: Isotropic hardening with modified stress-strain curve to simulate increased yield stress

The MAT protocol assumes that cold bending has occurred along the stress-strain path OABD in figure 5b, with a resulting plastic strain of OD. When the column is compressed, the stress-strain curve is then DBC, resulting in an apparent increased yield stress. The virgin stress-strain curve OAC was replaced with the curve DBC in ABAQUS (*MATERIAL definition) with the point D shifted to the origin (i.e., zero stress, zero strain).

4.3 ISO – Isotropic hardening including residual stresses and effective plastic strains

For the ISO modeling protocol, the residual stresses (in Cartesian stress space) and effective plastic strain (in von Mises strain space) were directly defined in ABAQUS (*INITIAL CONDITION definition) considering 99 sections (integration points) through the thickness. The residual stresses and plastic strain distributions, described in Figure 6 and Table 1, were obtained with the hand calculations described in [18]. Note that defining ε_p explicitly establishes the initial size of the von Mises yield surface, which is approximately equivalent to manually inputting the stress-strain curve DBC in the MAT protocol.

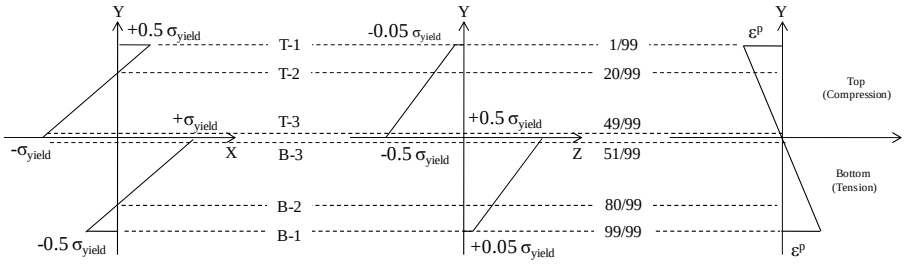

Figure 6: Residual stress and plastic strain distributions imposed in ABAQUS.

Table 1: Residual effective stresses and plastic strains at defined through-thickness section points.

	T-1	T-2	T-3	Center	B-1	B-2	B-3
σ_e . MPa	213.0	80.0	349.0	0.0	213.0	80.0	349.0
σ_1 . MPa	202.0	-39.0	-404.0	0.0	-202.0	39.0	404.0
σ_3 . MPa	-20.0	-92.0	-202.0	0.0	20.0	92.0	202.0
ε_p	0.11	0.068	0.0024	0	0.11	0.068	0.0024

4.4 COM – Isotropic-kinematic hardening including residual stresses and equivalent plastic strains

The COM protocol employs a combined isotropic-kinematic hardening law in ABAQUS and defines the initial size and location of the von Mises yield surface after cold bending. The size of the yield surface is established in the same way as Section 4.3 for the ISO protocol, i.e. with the user input of ε_p varying through the thickness.

The location of the yield surface requires the calculation of the backstress components $\Delta\sigma_1$ and $\Delta\sigma_3$:

$$\Delta\sigma_1 = \sigma_1^B - \sigma_1^A \tag{2}$$

$$\Delta\sigma_3 = \sigma_3^B - \sigma_3^A \tag{3}$$

The applied stress during cold bending, σ_1^B, is calculated from the effective plastic strain during cold bending:

$$\varepsilon_p^B = \frac{2}{\sqrt{3}} ln\left(1 + \left|\frac{Y}{r_z}\right|\right) \tag{4}$$

The effective stress, σ_e^B is read from OABC in figure 5b at a strain $\varepsilon = \varepsilon_{yield} + \varepsilon_p^B$ and then converted to σ_1^B by rearranging Eq. (1) and assuming $\sigma_3^B = \nu\sigma_1^B$ where ν=0.5 for plastic deformations [18, Appendix]:

$$\sigma_1^B = \frac{\sigma_e^B}{\sqrt{\nu^2 - \nu + 1}} \tag{5}$$

The stress components σ_1^A and σ_3^A in Cartesian space that result in $\sigma_e = \sigma_{yield}$ (point A in figure 5b) can be obtained by assuming $\sigma_3^A = \nu\sigma_1^A$, ν=0.3 for elastic deformation up to yield, and solving Eq. (1) for σ_1^A.

5 RESULTS AND DISCUSSION

The load-deformation response of the cold-bent compression member for the NORS, MAT, ISO and COM cases are compared in figure 7. The peak compressive load predicted by the MAT is approximately 40% higher than the baseline NORS protocol, simply because the stress-strain curve input into ABAQUS has a yield stress that is 40% higher than the virgin yield stress, σ_{yield}. The ISO protocol produces a similar load-deformation response to the MAT protocol with the effective plastic strain defining the initial size of the von Mises yield surface. The ISO curve softens at the yield knee because of the presence of the through-thickness residual stresses imposed as part of the initial state.

A more detailed look at the behavior of the cold-bent compression member when modeled with the ISO protocol is provided in figure 8a by tracking the effective (Mises) stresses, σ_e, through the loading sequence. The through-thickness stress magnitudes vary initially based on the residual stresses created by cold bending. As the compression load increases, the yield stress of the T-1 layer and its opposing layer B-1 are higher than the virgin yield stress (figure 8a), as every point on an ellipse in the σ_1 and σ_3 coordinate system (figure 9a) has the same yield stress. In other words, for isotropic hardening, the yield stress in opposing layers (e.g. T-1 and B-1) are increased by cold bending. The softening of the curve from MAT to ISO results from the residual stresses (σ_3) which place T-1, T-2, and T-3 in compression and B-1, B-2, and B-3 in tension. The variation in residual stresses results in a yield lag, with the B layers yielding later in analysis than the T layers.

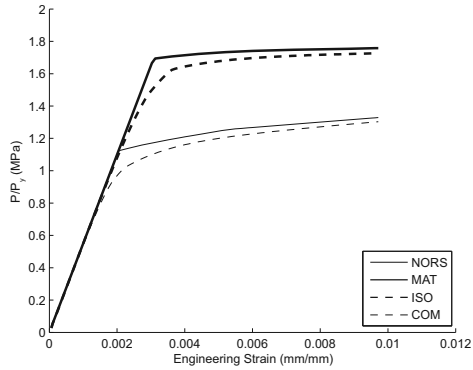

Figure 7: Cold-bent column load-deformation response. (Engineering strain on the *x*-axis is calculated as column shortening divided by the original column length.)

Returning to figure 7, it is observed that the COM modeling protocol (combined isotropic-kinematic hardening) is consistent with the baseline load-deformation response NORS, an interesting and unexpected result. Figure 8b demonstrates that a decrease in apparent yield stress occurs for all layers except T-3 and B-3. The decrease in yield stress results because of the combined effect of residual stresses and a shift in the yield surface (figure 9b). For example, the T-3 yielding surface shifts slightly as the plastic strain from cold bending is small near the center of the sheet thickness. However the σ_1

residual stresses from cold bending are near +0.50 σ_{yield} (figure 6b), and when the column is loaded in compression in the 3 direction, the distance to the yield surface is decreased when compared to loading from the origin O. It is concluded the COM load-deformation response is consistent with the NORS protocol because in most locations through the thickness the isotropic hardening effect, i.e. boost in yield stress, is partially to fully negated by the shifted yield surface and the presence of residual stresses.

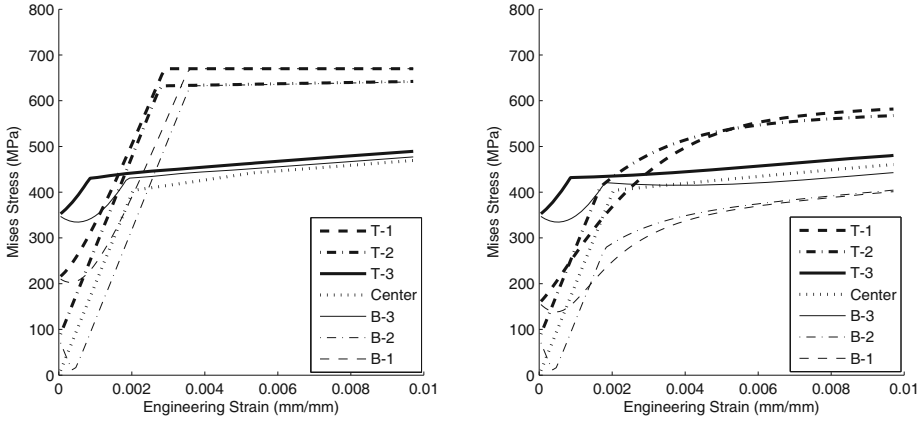

Figure 8: Effective (Mises) through-thickness stresses: (a) ISO protocol and (b) COM protocol.

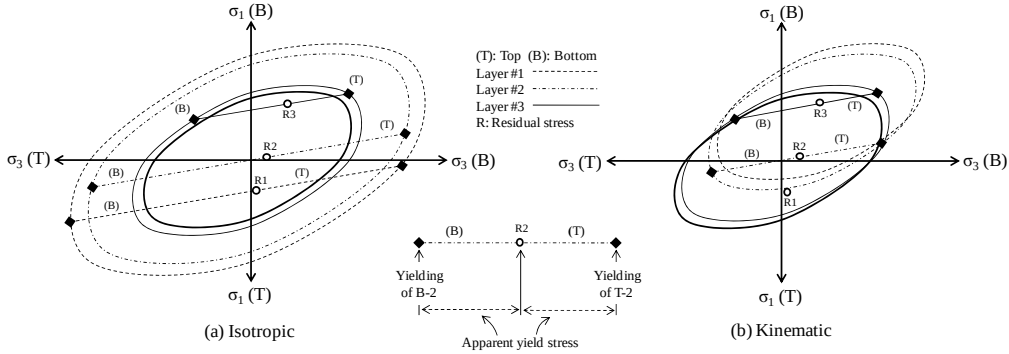

Figure 9: Through-thickness Mises yield surfaces: (a) ISO protocol and (b) COM protocol (note that only kinematic hardening is represented)

6 CONCLUSIONS

A nonlinear finite element parameter study considering residual stresses and plastic strains from cold bending demonstrates that load-deformation response is sensitive to the choice of metal plasticity law and the consideration of residual stresses and plastic strains. A combined isotropic-kinematic hardening law and user input residual stresses and effective plastic strains produce a load-deformation response consistent with the baseline case which ignores the effects of cold bending. The common finite element modeling practice of increasing the yield stress at the location of cold bending neglects to capture the yield lag from the presence of residual stresses and the shifting yield surface (i.e. the Bauschinger effect), and highlights that the current design treatment of an increased yield stress from the cold work of forming effect is inconsistent with the mechanics of cold bending.

REFERENCES

[1] Kloiber L. A., "Cambering of Steel Beams," American Society of Civil Engineers, 1989.

[2] Winters-Downey E., "Steel Wise "Specifying Camber"," American Instituite of Steel Construction, 2006.

[3] Packer J. A., Henderson J. E., *Hollow Structural Section: A Design Guide*. 2nd ed. Canadian Institute of Steel Construction, Alliston, Ontario, 1997.

[4] Chajes A., Britvec S. J., Winter G. "Effects of cold-straining on structural steel sheets," *Journal of the Structural Division, ASCE*, **89**(ST2), 1-32, 1963.

[5] Shanley F. R., *Strength of Materials*. McGraw-Hill Book Company, New York, NY, 1957.

[6] Key P., Hancock G. J. "A Theoretical Investigation of the Column Behaviour of Cold-Formed Square Hollow Sections," *Thin-Walled Structures*, **16**, 31-64, 1993.

[7] Weng C. C., Peköz T. "Residual Stresses in Cold-Formed Steel Members," *ASCE Journal of Structural Engineering*, **116**(6), 1611-25, 1990.

[8] De Batista E. M., Rodrigues F. C. "Residual stress measurements on cold-formed profiles," *Experimental Techniques*, **16**(5), 25-9, 1992.

[9] Spoorenberg R. C., Snijder H. H., Hoenderkamp J. C. D. "Experimental investigation of residual stresses in roller bent wide flange steel sections," *Journal of Constructional Steel Research*, **66**(6), 737-47, 2010.

[10] Quach W. M., Teng J. G., Chung K. F. "Finite element predictions of residual stresses in press-braked thin-walled steel sections," *Engineering Structures*, **28,** 1609-19, 2006

[11] Moen C. D., "Direct Strength Design for Cold-Formed Steel Members with Perforations," Ph.D. Thesis, Johns Hopkins University, 2008.

[12] Sivakumaran K. S., Abdel-Rahman N. "Finite element analysis model for the behaviour of cold-formed steel members," *Thin-Walled Structures*, **31**(4), 305-24, 1998.

[13] AISI-S100, *North American Specification for the Design of Cold-Formed Steel Structural Members*. American Iron and Steel Institute, Washington, D.C., 2007.

[14] Hancock G. J., Murray T., Ellifritt D., *Cold-formed steel structures to the AISI specification*. Marcel Dekker, Inc., New York, NY, 2001.

[15] Hill R., *The Mathematical Theory of Plasticity*. Oxford University Press, London, England, 1950.

[16] Quach W. M., Teng J. G., Chung K. F. "Residual stresses in steel sheets due to coiling and uncoiling: a closed-form analytical solution," *Engineering Structures*, **26,** 1249-59, 2004

[17] Ugural A. C., Fenster S. K., *Advanced Strength and Applied Elasticity, Fourth Edition*. Prentice Hall, Upper Saddle River, NJ, 2003.

[18] Moen C. D., Igusa T., Schafer B. W. "Prediction of Residual Stresses and Strains in Cold-Formed Steel Members," *Thin-Walled Structures*, **46**(11), 1274-89, 2008.

[19] ABAQUS, "ABAQUS/Standard Version 6.9-2.," Dassault Systèmes, <http://www.simulia.com/>, 2009.

[20] Chen W. F., Han D. J., *Plasticity for Structural Engineers*. Springer-Verlag, New York, NY, 1988.

[21] Ramm E., "Strategies for tracing nonlinear response near limit points," Springer, 1981.